Int J Wireless Inf Networks
DOI 10.1007/s10776-014-0236-x

Closed Loop Power Control Using Third Order Quadratic Approximator

Andre M. Mayers · Patrick J. Benavidez · G. V. S. Raju · David Akopian · Mo M. Jamshidi

Received: 1 April 2013 / Accepted: 3 February 2014

Abstract In this paper we introduce a novel bit error rate (BER) feedback transmit power control (TPC) system using a first-time third order quadratic approximation of the power–time curve. This approximation improves the power efficiency of a dual-rate TPC algorithm in terms of reduced total transmit power by smoothing transmit power transients during adaptive iterations. We show that the third order approximator outperforms linear and second order approximators in terms of transmit power savings, sensitivities, error magnitude, and better tracking performance in following reference desired power curves. For the approximator, we determine operational bounds for stability, and demonstrate algorithm behavior using critical valued inputs. In addition we demonstrate value in using a dynamic, rather than static, performance benchmark for quality of service approximation (obtained used scaled maximum acceptable BER), and provide heuristic estimates for the input parameters for the dynamic benchmark.

Keywords Cognitive radio · Transmit power control · Interference avoidance · Quadratic approximator · Power usage efficiency

1 Introduction

Cognitive radio (CR) devices often opportunistically access the wireless spectrum [1, 2], and as such, must practice interference avoidance through various energy efficiency techniques (IA) e.g. [3, 4]. For example, wireless CR PAN devices tend to operate in short range, low power communications and use technologies such as WiMedia, Bluetooth, and ultra-wideband, UWB [5]. The authors consider it important to develop a technology-agnostic interference avoidance technique that is responsive to quality of service (QoS) requirements such as maintaining acceptable bit error rate (BER). In this paper, we use the energy efficiency approach of employing a transmit power control (TPC) system for wireless CR devices using a novel, first time third order quadratic approximation of the power–time curve, called the BER–TPC. This paper addresses the power efficiency of adaptive TPC in terms of reduced total transmit power of the network by smoothing transmit power transients during adaptive iterations using a novel, first time third order quadratic approximation of the power–time curve. We also advance the quadratic approximator approach by implementing this system using algorithms at both constituents (transmitting and receiving) of the communication system instead of only at the transmitter [6].

In theory, there is an optimal power–time curve reflective of the minimum amount of power necessary with which communicating systems can transmit while maintaining acceptable BER. We seek to model this curve using heuristically estimated dual-rate power adjustments during adaptive iterations. A very important aspect of the dual-rate adjustment is a dynamic benchmark with the initial value a scaled maximum acceptable BER. As maximum acceptable BERs are device specific, the algorithm is tailored to maintain required BERs. We show that the dynamic benchmark is superior to a static one, and introduce heuristically obtained input parameters for manipulation of the operation of this benchmark. Because transmit power is adjusted using a mathematical formula, it is trivial to obtain operational bounds for stability, robustness, to calculate the

A. M. Mayers (✉) · P. J. Benavidez · G. V. S. Raju · D. Akopian · M. M. Jamshidi
The University of Texas at San Antonio, San Antonio, TX, USA
e-mail: andremayers@yahoo.com

Published online: 21 February 2014

rate of power adjustment, and impose limits on transmit power.

Feedback approaches for power control have already been used in state-of-the-art approaches such as in [7–9], in which signal-to-interference-plus-noise ratio (SINR) estimations are used. In [10], the authors establish bounds on the practicability of the CR channel sensing feedback in power control when outage constraints for licensed users are a consideration. In [8], the authors use SINR feedback for a joint strategy on power control and radio channel allocation, subject to constraints on transmission power and data traffic rates.

One feedback-based TPC algorithm is proposed in [11] called the distributed power controller (DPC). The DPC uses the proportional integral derivative (PID) controller concept that produces a stable system and is used to adaptively tune PID gains. The controller input is the difference between actual received SINR and target SINR determined by QoS requirements.

However, according to the authors of [12], in weak signal environments, the SINR feedback-based methods have the issue of being constrained by some inaccuracy of SINR estimates. Therefore, in the proposed system, SINR feedback is replaced with BER measurements obtained from pilot subcarriers. The data in received pilot arrays are compared to expected data to estimate BERs. The receiver compares current BER with maximum BER allowed and sends a binary signal to the transmitter indicative of acceptable or unacceptable BER. In addition, the proposed controller is different from PID and is tailored to a BER-based feedback system.

One should also note that the proposed system reduces the transmission power for an active established link. Because the proposed method is technology-agnostic, it can be integrated with extant power saving techniques e.g. in sensor networks exploiting duty cycling by switching off the power during periods of inactivity [13], with techniques employing data reduction through exploiting spatial or temporal correlation [14], techniques utilizing optimization of routing paths [15–17], in trading off modes of operation in large scale, high density, high mobility wireless sensor networks for increased energy efficiency.

The layout of the paper is as follows. In Sect. 2, we describe the system model and control parameters. In Sects. 3 and 4, we develop and compare the first, second, and third order approximators in terms of overshoot and damping. Finally, we submit results, including comparison with SNR controllers, and close with conclusions.

2 System Model and Control Parameters

The system includes one or more licensed or primary users (PUs), and several interoperable secondary users (SUs). The power control system operates separately for each communicating pair of PAN devices. We stipulate that our PADs devices use CR technology [18, 19] and we use the WiMedia Alliance multiband orthogonal frequency division multiplexing (MB-OFDM) UWB system [20]. This paper accepts the SDCR approach for applying the proposed power adaptation technique [21]. Below, we present the control parameters and their operation in the first, second, and third order approximators.

2.1 Control Parameters $[R_e^F(k),\ R_e^D(k),\ R_e^M]$ at Receiver

At the receiver, $R_e^F(k)$ is the mean of the BER in the MB-OFDM pilot subcarriers. $R_e^F(k)$ is compared to R_e^M, the maximum acceptable BER (usually manufacturer defined) for a SU, and we obtain

$$R_e^d(k) = \left\{ \begin{array}{c} 1,\ \text{if } R_e^F(k) \le R_e^M \\ -1,\ \text{if } R_e^F(k) > R_e^M \end{array} \right\}, \tag{1}$$

which is sent to the transmitter.

2.2 Control Parameters $[\lambda(k),\ R_e^{F_s}(k),\ e_o(k)]$ at Transmitter

At the transmitter, parameter $R_e^{F_s}(k)$ is called the *memory-based feedback index* and is a function of BER feedback, while $\lambda(k)$ is a dynamically adjusted benchmark. At initialization, $R_e^{F_s}(0) = \lambda(0) = (s * R_e^M)^{-1}$, where s is a scaling factor. $R_e^{F_s}(k)$ is iteratively updated using

$$R_e^{F_s}(k) = R_e^{F_s}(k-1) + R_e^d. \tag{2}$$

The parameter $\lambda(k)$ is defined in an iterative manner as

$$\lambda(\tau) = \left\{ \begin{array}{c} \lambda(\tau-1) - 1,\ \text{if } \lambda^C(k) > \lambda^T \\ \lambda(\tau-1) + 1,\ \text{if } \lambda^C(k) < -\lambda^T \end{array} \right\}, \tag{3}$$

where $\lambda^C(k)$ is an initialized counter and λ^T is an integer threshold that, when crossed triggers an adjustment in $\lambda(k)$. $\lambda^C(0) = 0$, and is reset to zero when either of the cases described in (5) are satisfied. It is updated using

$$\lambda^C(k) = \left\{ \begin{array}{c} \lambda^C(k-1) + 1,\ \text{if } R_e^F(k) \ge R_e^M \\ \lambda^C(k-1) - 1,\ \text{if } R_e^F(k) < R_e^M \end{array} \right\}. \tag{4}$$

In the BER feedback power control (BER–TPC) algorithm, the control error, $\hat{e}(k)$ is defined by

$$\hat{e}(k) = \lambda(k) - R_e^{F_s}(k), \tag{5}$$

and determines the magnitude of the increase/decrease in transmit power.

2.3 Approximators $\alpha_1(k),\ \alpha_2(k),\ \alpha_3(k) = f(R_e^{F_s}(k),\ \lambda(k),\ e_o(k))$

In this subsection, we introduce the control approximators, $\alpha_1(k)$, $\alpha_2(k)$, $\alpha_3(k)$. The $\alpha_1(k)$ linear control parameter is obtained by tuning or normalizing $e_o(k)$, using the dynamically adjusted benchmark, $\lambda(k)$. However, in light of the theoretically approachable time versus power curve, we can cite Taylor's theorem, which states that if a function f is differentiable at point a, then it has a linear approximation at that point. To reduce the error in the approximation, we use quadratic second and third order approximators by normalizing $e_o(k)$ using $\lambda(k)^2$, $\lambda(k)^3$ as in (7) and (8).

$$\begin{aligned}&\text{(a) } \alpha_1(k) = 1 - \frac{\hat{e}(k)}{\lambda(k)} = 2 - \frac{R_e^{F_s}(k)}{\lambda(k)},\\ &\text{(b) } 0 < \lambda(k), \quad \lambda(k) \neq 0.5 * R_e^{F_s}(k),\end{aligned} \tag{6}$$

$$\begin{aligned}&\text{(a) } \alpha_2(k) = 1 + \frac{\hat{e}_o(k)}{\lambda(k)^2} = 1 + \frac{\lambda(k) - R_e^{F_s}(k)}{\lambda(k)} = 2 - \frac{R_e^{F_s}(k)}{\lambda(k)^2},\\ &\text{(b) } 0 < \lambda(k) < 2 * R_e^{F_s}(k),\\ &\text{(c) } \lambda(k) \neq -0.5 \pm\ > 0.5 * \sqrt{1 + 4 * \left(R_e^{F_s}(k)\right)},\end{aligned} \tag{7}$$

$$\begin{aligned}&\text{(a) } \alpha_3(k) = 1 + \frac{\lambda(k) - R_e^{F_s}(k)}{\lambda^3(k)} = 1 + \frac{1}{\lambda^2(k)} - \frac{R_e^{F_s}(k)}{\lambda^3(k)},\\ &\text{(b) } 0 < \lambda(k) < 1.5 * R_e^{F_s}(k).\end{aligned} \tag{8}$$

An important contribution of quadratic approximations is that they can be mathematically examined in terms of stability and operational range. We stipulate $R_e^{F_s}(k)$ is unbounded, and assume stability in (6a), (7a), (8a) by constraining $\lambda(k)$ to avoid poles and zeros using (6b), (7b, c), and (8b), respectively. We determine the operational range of $\alpha_{1,2,3}(k)$ by observing the conditions over which $\alpha_o(k)$ is monotonic.

2.4 Power Control, BER–TPC and Comparative PID Algorithms

Transmit power is, therefore, adjusted using

$$P_T^{SU} = \overrightarrow{P}(k)^{\alpha(k)}, \tag{9}$$

where P_T^{SU} is the total power in a MB-OFDM band, and $\vec{P}(k)$ is a vector of the power profile in the band, before power adjustment. The aim of the BER–TPC algorithm is to minimize P_T^{SU} through iterative adjustment of $\lambda(k)$, $R_e^{F_s}(k)$, while satisfying the constraints

$$\begin{aligned}&\sum_{i=1}^{M}\sum_{j=1}^{128} h_{i,j}P_i + P_T^{SU} \leq S_{\max},\\ &R_e^{SU} \leq R_e^{M},\end{aligned} \tag{10}$$

where R_e^{SU} is the SUs mean BER over the life of the transmission. An important contribution is that an upper limit on transmit power is deterministic using

$$R_{\lim}^{F_s}(k) = \lambda(k)\left[1 - \frac{\lambda(k)(-\ln(P(k))) + \ln\left(P_{\max}^{SU}(k)\right)}{\ln(P(k))}\right], \tag{11}$$

where $R_{\lim}^{F_s}(k)$ is a lower limit on the value of $R_e^{F_s}(k)$ and $P_{\max}^{SU}(k)$ is a dynamic limit on SU transmit power. For example, (11) is the limit on the second order approximator (7).

2.5 Comparison of First, Second, and Third Order Approximators in Terms of Overshoot, Damping

We perform the comparison of the three orders approximator in the calculation of $\alpha_o(k)$ as follows. We introduce $R_{e,\min}^{F_s}$ as the minimum acceptable value for $R_e^{F_s}(k)$. We also introduce $d_{\max,R_e^{Fs}(k),\lambda(k)}$, which we define as the maximum possible deviation (dependent upon the *dpi* value) between $R_e^{F_s}(k)$ and $\lambda(k)$. Let us define a dynamic range for $R_e^{F_s}(k)$ and place further restrictions on $R_e^{F_s}(k)$, $R_{e,\min}^{F_s}$:

$$R_e^{F_s}(k) \in \left[\lambda(k) - d_{\max,R_e^{Fs}(k),\lambda(k)},\ \lambda(k) + d_{\max,R_e^{Fs}(k),\lambda(k)}\right], \tag{12}$$

$$R_{e,\min}^{F_s} = -d_{\max,R_e^{Fs}(k),\lambda(k)}, \tag{13}$$

$$R_e^{F_s}(k) \in \left(R_{e,\min}^{F_s},\ \infty\right]. \tag{14}$$

Because the lower bound for $\lambda(k)$ is 0, we can obtain a lower bound for (12) and (14). Stability of error exponent approximation is ensured provided by the design rules and assumptions (i–iv), which provide bounded inputs and outputs:

(i) Restriction in (12) provides acceptable oscillation magnitude in calculation of $\alpha_{1,2,3}(k)$ due to low sensitivity to $R_e^{F_s}(k)$.

(ii) Assumption: Eqs. (12) and (14) are always true due to channel diversity and optimal channel switching in OFDM. As BER on one channel decreases, another channel may be switched too, depending on BER and other criteria.

(iii) Assumption: given that $\lambda(k)$ tracks $R_e^{F_s}(k)$ by the dynamic range restrictions in (12), $\alpha_{1,2,3}(k) \cong 1$ as subject to the statement in (i). As $R_e^{F_s}(k)$ is

approximately equal to the value of with maximum deviation the value is always approximately equal to 1.

(iv) Communication transceivers actual capabilities are limited by the receiver sensitivity and transmitter power; therefore, maximum and minimum values of $\alpha_{1,2,3}(k)$, $\lambda(k)$, and $R_e^{F_s}(k)$ are already set by physical conditions and limits of the transceiver.

We introduce the *ideal conditions* of the approximator as $\alpha_o(k) = 1$, where the power output is equal to the required power output based on the BER feedback $R_e^F(k)$. Furthermore, behavior of the approximator's operation near critical points at poles of $\alpha_o(k)$ function is described by the following:

$R_e^{F_s}(k) \approx R_{e,\min}^{F_s}$:

(i) $\Delta\alpha_o(k)$ is large in the first order approximator due to the $1/\lambda(k)$ term.

(ii) $\Delta\alpha_o(k)$ in second and third order approximators are reduced greatly as compared to the first order approximator.

$R_e^{F_s}(k) \gg R_{e,\min}^{F_s}$:

(iii) $\Delta\alpha_o(k)$ is larger for the first order approximator than the second and third order approximators, but smaller in scale than that in case (i).

(iv) $\Delta\alpha_o(k)$ is small for second and third order approximators.

We evaluate the approximator performance with conditions given in (11), (13) and (14) for first, second, and third order versions of error exponent approximations for $\alpha_1(k)$, $\alpha_2(k)$, $\alpha_3(k)$ (Eqs. (6)–(8), respectively), and present the following conclusions on approximator performance. The first order approximator has larger overshoot tracking the "ideal" line with $\alpha_o(k)$ underdamped. The second order approximator has significantly reduced overshoot, $\alpha_o(k)$ is damped, and tracks the "ideal" line well with fast convergence. Third order converges quickest and tracks the "ideal" line with minimal overshoot, with $\alpha_o(k)$ damped.

2.6 Overview and Model of BER–TPC System

Figure 1 is a block diagram model of the BER–TPC system. At the receiver, BER feedback is calculated at the pilot channel data comparator and passed to the BER feedback thresholder where it is compared to the maximum acceptable BER. The result value $R_e^d(k) = \pm 1$ is sent to the transmitting CR. There, using the dynamic benchmark adjustor and the instantaneous adjustor, $\lambda(k)$ and $R_e^{F_s}(k)$ are respectively updated. The error $\hat{e}(k)$ is calculated and sent to the controller calculator, which results in an updated $\alpha(k)$, which, along with the pre-adjusted power vectors $[\vec{P}(k)]$ is used to obtain the new power update.

3 Results and Simulations

The Monte Carlo method was used and simulation parameters are as follows: modulation QPSK, attenuation and path loss are assumed to be negligible, 14 MB-OFDM bands with bandwidth of 528 MHz, each 128 OFDM subcarriers, data rate 3 Mbit/s, transmitted data 4 Mb, subcarrier interference (PU) power is generated using a continuous uniform distribution over a range of −0 to

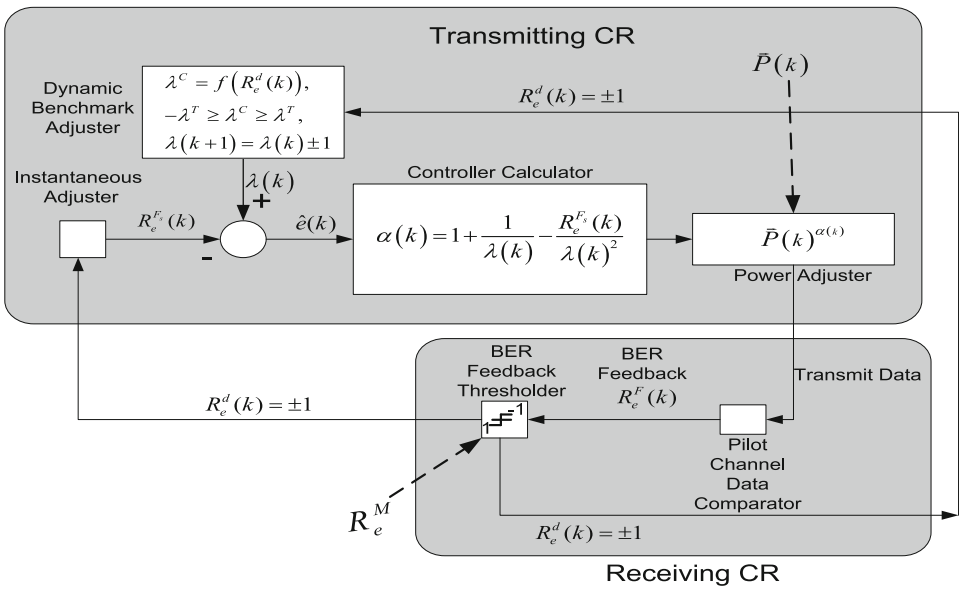

Fig. 1 Block diagram of approximator transmit power control system

Table 1 Comparison of PID and SNR controllers to the second order BER–TPC in terms of BER and transmit PSD, expressed in dB

	C(DPC)	*C*(SNR)	First order	Second order
BER (dB)	+5.65	+7.12	+11.4	+0.7
PSD (dB)	+3.5	−2.6	+9.7	+1.8

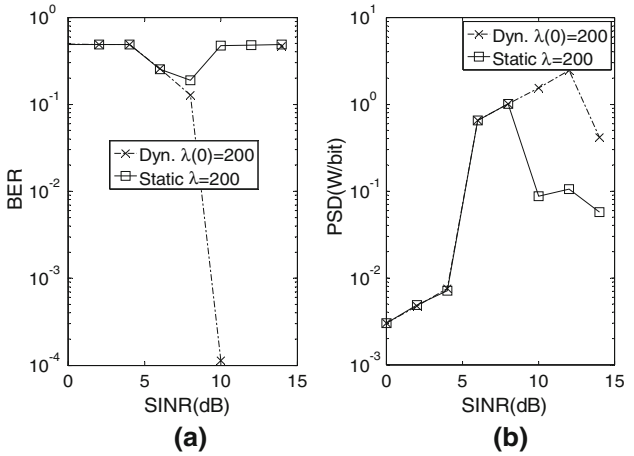

Fig. 2 Effect of dynamic benchmark ($\lambda(0) = 200$) versus static benchmark ($\lambda = 200$) on **a** BER, and **b** transmit PSD (W/Hz)

30.3 dBm, S_{max} 47–49 dBm, $10e-6 \leq R_M^e \leq 10e-3$. Typical OFDM transmission is used, except the power control method is applied after band and subcarrier selection, and before modulation and bit loading. In all simulations, BER is the BER in the data carrying subcarriers.

Table 1 compares the performance of the *C*(DPC), *C*(SNR) [9], first and third order with the second order approximator. The control parameters for the DPC controller, *C*(DPC), are $\partial = 0$, $\beta = -1$, $\theta = 1$. In terms of BER, the third order approximator exhibits superior performance to all other controllers. In terms of transmit power, the SNR controller is the only one that outperforms the third order approximator. When both metrics are taken into account, we conclude the third approximator is the best performer under the stated conditions.

Figure 2 shows (a) BER and (b) transmit PSD for a static $\lambda = 200$ versus dynamically adjusted benchmark with $\lambda(0) = 200$, using the third order approximator. The static benchmark is unchanging. The dynamic benchmark is adjusted if BER feedback is either consistently above or below maximum acceptable BER. This produces a tuning effect in that it affects the size of the increments of transmit power adjustments. Results indicate that the dynamic benchmark is preferable to the static one because it is more responsive to QoS (in this case BER). This can be observed in that while the transmit PSD is better (lower) with the

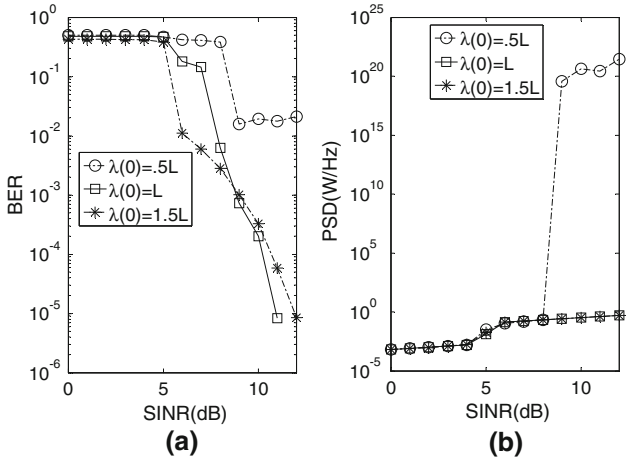

Fig. 3 Effect of three different dynamic benchmark initialization values on **a** BER, and **b** transmit PSD for $\lambda(0) = 0.5 * L$, L, and $1.5 * L$, $L = 400$

static benchmark for SINR >7 dB, BER is unacceptably high, indicating lack of responsiveness.

The results in Fig. 3 demonstrate the importance of the device specific initial value for $\lambda(k)$, derived from device specific maximum acceptable BER (recall $\lambda(0) = (s * R_e^M)^{-1}$). In Fig. 3, the correct initial value $\lambda(0) = L = 400$, is compared in terms of (a) BER and (b) transmit PSD to $\lambda(0) = 0.5L$, and $1.5L$. The results indicate that for best performance transmit power adjustment should be done with initial benchmark values at least equal to the actual value. This ensures fine grained tuning as opposed to smaller values of $\lambda(0)$, which result in coarse grained tuning and, thus, very high transmit PSD.

In Fig. 4, we compare the effects of $\lambda^T = 0.3B$, B, $2B$, $B = 6$, using (a) BER and (b) transmit PSD. Recall λ^T is used in determining when long-term BER feedback trends are used to dynamically adjust power tuning by incrementing/decrementing the value of $\lambda(k)$. From observation of this figure, and similar results obtained using Monte Carlo methods, we recommend $\lambda^T \geq 6$ because smaller values lead to undesirable fluctuations in increment/decrement step size, resulting in coarse grained tuning.

Figure 5a shows the approximators' BER error magnitude (EM) deviation from (maximum acceptable BER) $R_e^M = 2 \times (10^{-3})$ for iterations 1–k, while Fig. 5b zooms in showing $(k - x)$–k, $x = 100$. These two figures show that the quadratic approximators' performances are consistent, with best responsivity, and smoothest tracking from the third order, clearly shown in Fig. 5b. It is obvious, however, that the first order approximator EM is undamped.

Figure 6a shows the BER performance of the three approximators in comparison with R_e^M. The quadratic approximators vastly outperform the linear (first order) approximator, with the third order performing best in maintaining BER below or near R_e^M. Performance between

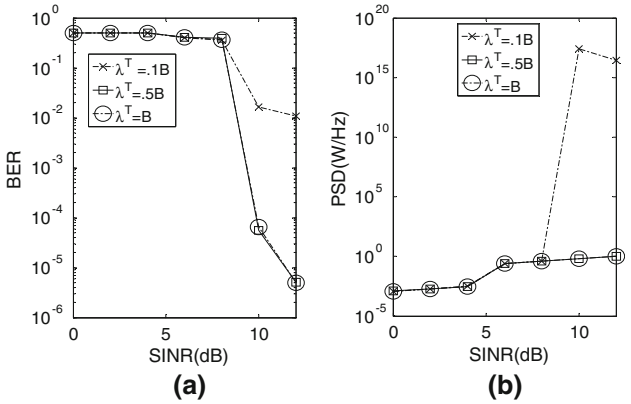

Fig. 4 Effect of three different dynamic benchmark threshold values on **a** BER, and **b** transmit PSD (W/Hz) for $\lambda^T = 0.5 * B$, B, and $2 * B$, $B = 6$

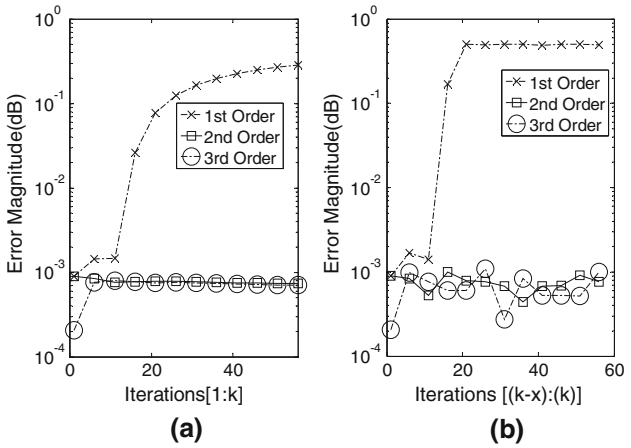

Fig. 5 Comparison of error magnitude for first, second, third order BER–TPC approximators, for **a** iterations 1–(k) (to demonstrate long term behavior), and **b** iterations ($k-1$)–(k) (to demonstrate instantaneous response) to BER feedback

the second and third order is similar, however, the third order has a slightly smaller variance, indicating smoother transients between adaptive iterations. Figure 6b shows variance of transmit PSD where the third order approximator outperforms the second order approximator by 0.3 dB. Taking BER, EM and transmit power savings into consideration, we conclude that the third order approximator is the best performer.

4 Conclusions

In this paper, we proposed a power control system that uses a quadratic approximation of the power–time curve for devices that opportunistically access the wireless spectrum.

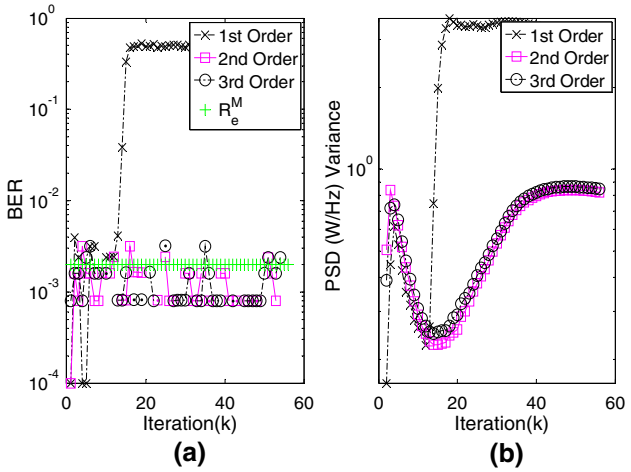

Fig. 6 Comparison of first, second and third order approximators' effect tracking maximum acceptable BER ($R_e^M = 2e-3$)on **a** BER and **b** PSD (W/Hz) variance over k iterations

It was our goal to reduce total transmit power of a CR network by, for each device, smoothing transmit power transients during adaptive iterations. This is achieved using a distributed closed loop power control system that applies heuristically estimated dual-rate power adjustments during adaptive iterations. Because of the non-linear channel conditions and at times forced compliance with caps on interference to licensed devices, we attempted to introduce a highly dynamic, responsive, yet stable approach. We showed that dynamic (BER) benchmark adjustments exhibit superior performance to a static benchmark, introduced operational ranges for the approximators' parameters, and based on transmit PSD variance, BER, and EM deviation from acceptable BER, determined that the third order approximator performs best under the specified conditions. We also demonstrated superior performance in transmit PSD reduction to conventional SNR feedback-based controllers. Because the proposed method is technology-agnostic, it can be integrated with extant power-saving techniques such as duty cycling, efficient routing, etc.

Acknowledgments This work was supported in part by NSF Grants 0942852, 0932339 and CRI-0551501.

References

1. T. Zahariadis, Personal area networks, *Communications Engineering*, Vol. 1, No. 3, pp. 12–15, 2003.
2. M. Chen, S. Gonzalez, A. Vasilakos, H. Cao, and V. C. M. Leung, Body area networks: a survey, *Mobile Networks and Applications*, Vol. 16, No. 2, pp. 171–193, 2010.
3. E. Dall'Anese, S.-J. Kim, G. B. Giannakis, and S. Pupolin, Power control for cognitive radio networks under channel uncertainty,

IEEE Transactions on Wireless Communications, Vol. 10, No. 10, pp. 3541–3551, 2011.
4. M. I. Razzak, B. A. Elmogy, M. K. Khan, and K. Alghathbar, Efficient distributed face recognition in wireless sensor network, *International Journal of Innovative Computing, Information and Control*, Vol. 8, No. 4, pp. 2811–2822, 2012.
5. H.-B. Li, and R. Kohno, Body area network and its standardization at IEEE 802.15. BAN, in *Advances in Mobile and Wireless Communications*, Springer, Berlin, 2008, pp. 223–238.
6. A. Mayers, P. Benavidez, G. Raju, D. Akopian, and M. Jamshidi, A novel BER-feedback power control algorithm for Personal Area Network Devices, in *Systems Conference* (*SysCon*), *2013 IEEE International*, 2013, pp. 370–375.
7. E. C. Peh, Y.-C. Liang, and Y. Zeng, Sensing and power control in cognitive radio with location information, in *2012 IEEE International Conference on Communication Systems* (*ICCS*), 2012, pp. 255–259.
8. M. Yu, X. Ma, W. Su, and L. Tung, A new joint strategy of radio channel allocation and power control for wireless mesh networks, *Computer Communications*, Vol. 35, No. 2, pp. 196–206, 2012.
9. N. Hoven, and A. Sahai, Power scaling for cognitive radio, in *2005 International Conference on Wireless Networks*, *Communications and Mobile Computing*, vol. 1, 2005, pp. 250–255.
10. G. Anastasi, M. Conti, M. Di Francesco, and A. Passarella, Energy conservation in wireless sensor networks: a survey, *Ad Hoc Networks*, Vol. 7, No. 3, pp. 537–568, 2009.
11. A. Paul, M. Akar, M. G. Safonov, and U. Mitra, Adaptive power control for wireless networks using multiple controllers and switching, *IEEE Transactions on Neural Networks*, Vol. 16, No. 5, pp. 1212–1218, 2005.
12. R. Tandra, and A. Sahai, SNR walls for signal detection, *IEEE Journal of Selected Topics in Signal Processing*, Vol. 2, No. 1, pp. 4–17, 2008.
13. S. Jin, W. Yue, and Q. Sun, Performance analysis of the sleep/wakeup protocol in a wireless sensor network, *International Journal of Innovative Computing Information and Control*, Vol. 8, No. 5, pp. 3833–3844, 2012.
14. M. C. Vuran, Ö. B. Akan, and I. F. Akyildiz, Spatio-temporal correlation: theory and applications for wireless sensor networks, *Computer Networks*, Vol. 45, No. 3, pp. 245–259, 2004.
15. C. Han, T. Harrold, S. Armour, I. Krikidis, S. Videv, P. M. Grant, H. Haas, J. S. Thompson, I. Ku, and C.-X. Wang, Green radio: radio techniques to enable energy-efficient wireless networks, *IEEE Communications Magazine*, Vol. 49, No. 6, pp. 46–54, 2011.
16. A. Papadopoulos, A. Navarra, J. A. McCann, and C. M. Pinotti, VIBE: an energy efficient routing protocol for dense and mobile sensor networks, *Journal of Network and Computer Applications*, Vol. 35, No. 4, pp. 1177–1190, 2012.
17. S. Videv, and H. Haas, Energy-efficient scheduling and bandwidth-energy efficiency trade-off with low load, in *2011 IEEE International Conference on Communications* (*ICC*), 2011, pp. 1–5.
18. N. Devroye, M. Vu, and V. Tarokh, Cognitive radio networks, *IEEE Signal Processing Magazine*, Vol. 25, No. 6, pp. 12–23, 2008.
19. S. Haykin, Cognitive radio: brain-empowered wireless communications, *IEEE Journal on Selected Areas in Communications*, Vol. 23, No. 2, pp. 201–220, 2005.
20. A. Batra, S. Lingam, and J. Balakrishnan, Multi-band OFDM: a cognitive radio for UWB, in presented at the *Conference Proceeding of IEEE International Symposium on Circuits and Systems* (*ISCAS*), 2006, pp. 4094–4097.
21. V. D. Chakravarthy, Z. Wu, A. Shaw, M. A. Temple, R. Kannan, and F. Garber, A general overlay/underlay analytic expression representing cognitive radio waveform, in *2007 International Waveform Diversity and Design Conference*, 2007, pp. 69–73.

Andre M. Mayers received the BSc Degree in Computer Science from North Carolina Central University, USA in 2002, and completed the MSc Degree in Electrical Engineering the University of Texas at San Antonio (UTSA), USA in 2009. Currently he is a PhD student in the Software Communications and Navigations Systems Laboratory (SCNS) Laboratory in the electrical and computer engineering program at UTSA. His research interests include control systems, interference mitigation and avoidance in RF channels, sensor localization, and ad hoc networks.

Patrick J. Benavidez received the BSc Degree in Electrical Engineering from The University of Texas at San Antonio, USA in 2007, and the MSc Degree in Electrical Engineering the University of Texas at San Antonio (UTSA), USA in 2010. Currently he is a PhD student in the Autonomous Control Engineering (ACE) Laboratory in the electrical and computer engineering program at UTSA. His research interests include robotics, control systems, wireless networks, soft computing, and RGB-D cameras. He has been involved in the organization of the 2013 World Conference on Soft Computing (WCSC) and student conferences at UTSA.

G. V. S. Raju M'67–SM'79 received the PhD in Electrical Engineering from the Polytechnic Institute of Brooklyn, Brooklyn, NY in 1965. He was Professor and Chairman of the Electrical and Computer Engineering Department at Ohio University from 1973 to 1984. From 1985 to 1987, he was a Visiting Professor at the Artificial Intelligence Robotics Laboratory, Computer Science Department, at Stanford University. He was Professor and Director of The Division of Engineering at the University of Texas at San Antonio. He has published widely in the areas of robotics, computer vision, adaptive control, fuzzy logic control and nuclear reactor control. He was President of the IEEE Systems, Man, and Cybernetics Society for the years 1986 and 1987. He retired as the Peter T. Flawn Distinguished Professor at The University of Texas at San Antonio (UTSA). He is a Life Fellow of IEEE and he received MILLENNIUM MEDAL from IEEE in 2000. Over the years he was an investigator, co-PI and PI to multimillion dollar grants from NASA, DoD, FAA, DoE, NSF and industry. With this extramural

funding, he was able to conduct basic theory and applied research in the areas of Computer Communications Networks, networks security, wireless communications and intelligent systems. He is the author of numerous technical publications in refereed journals and peer-reviewed conference proceedings. He is listed in American Men and Women in Science, Who's Who in America, the Dictionary of International Biography, and Outstanding Intellectuals of twenty first century.

David Akopian M'02–SM'04 is an Associate Professor at the University of Texas at San Antonio (UTSA). Prior to joining UTSA he was a Senior Research Engineer and Specialist with Nokia Corporation from 1999 to 2003. From 1993 to 1999 he was a Member of teaching and research staff of Tampere University of Technology, Finland, where he also received the PhD Degree in Electrical Engineering. Dr. Akopian's current research interests include digital signal processing algorithms for communication and navigation receivers, positioning, dedicated hardware architectures and platforms for software defined radio and communication technologies for healthcare applications. He authored and co-authored more than 30 patents and 120 publications. He served in organizing and program committees of many IEEE conferences and co-chairs annual SPIE Multimedia on Mobile Devices conference. His research has been supported by National Science Foundation, National Institutes of Health, USAF, US Navy and Texas Higher Education Coordinating Board.

Mo M. Jamshidi Fellow IEEE, Fellow ASME, A. Fellow-AIAA, Fellow AAAS, A. Fellow TWAS, Fellow NYAS, Member HAE received BS in EE, Oregon State University, Corvallis, OR, USA in June 1967, the MS and PhD Degrees in EE from the University of Illinois at Urbana-Champaign, IL, USA in June 1969 and February 1971, respectively. He holds Honorary Doctorate Degrees from University of Waterloo, Canada, 2004 and Technical University of Crete, Greece, 2004 and Odlar Yourdu University, Baku, Azerbaijan, 1999. Currently, he is the Lutcher Brown Endowed Distinguished Chaired Professor at the University of Texas, San Antonio, TX, USA. He has been an Advisor to NASA (including 1st MARS Mission), USAF Research Laboratory, USDOE and EC/EU (Brussels). He has advised over 60 MS and nearly 50 PhD students. He has over 680 technical publications including 68 books (12 text books), research volumes, and edited volumes in English and a few foreign languages. He is the Founding Editor or Co-founding Editor or Editor-in-Chief of five journals including IEEE Control Systems Magazine and the IEEE Systems Journal. He is an Honorary Professor at Deakin University (Australia), Birmingham University (UK), Obuda University (Hungary), and at three Chinese Universities (Nanjing and Xi'an, China). He has received numerous honors and awards, including IEEE Centennial Medal, IEEE Millennium Awards, and the IEEE's Norbert Weiner Research Achievement Award, among others. He is a Member of the University of the Texas System Chancellor's Council since 2011. He is currently involved in research on system of systems engineering with emphasis on cloud computing, robotics, UAVs, biological and sustainable energy systems, including smart grids.